Exciton-Coupled Charge-Transfer Dynamics in a Porphyrin J-Aggregate/TiO2 Complex

ARTICLE *in* CHEMISTRY - A EUROPEAN JOURNAL · MARCH 2011

Impact Factor: 5.73 · DOI: 10.1002/chem.201002537 · Source: PubMed

4 AUTHORS:

Sandeep Verma
Bhabha Atomic Research Centre
35 PUBLICATIONS **619** CITATIONS
SEE PROFILE

Amrita Ghosh
Central Salt and Marine Chemicals Researc…
33 PUBLICATIONS **803** CITATIONS
SEE PROFILE

Amitava Das
CSIR - National Chemical Laboratory, Pune
195 PUBLICATIONS **4,722** CITATIONS
SEE PROFILE

Hirendra N Ghosh
Bhabha Atomic Research Centre
127 PUBLICATIONS **3,859** CITATIONS
SEE PROFILE

CHEMISTRY
A EUROPEAN JOURNAL

DOI: 10.1002/chem.201002537

Exciton-Coupled Charge-Transfer Dynamics in a Porphyrin J-Aggregate/TiO_2 Complex

Sandeep Verma,[a] Amrita Ghosh,[b] Amitava Das,[b] and Hirendra N. Ghosh*[a]

Abstract: Exciton-coupled charge-transfer (CT) dynamics in TiO_2 nanoparticles (NP) sensitized with porphyrin J-aggregates has been studied by femtosecond time-resolved transient absorption spectroscopy. J-aggregates of 5,10,15-triphenyl-20-(3,4-dihydroxyphenyl) porphyrin (TPPcat) form CT complexes on TiO_2 NP surfaces. Catechol-mediated strong CT coupling between J-aggregate and TiO_2 NP facilitates interfacial exciton dissociation for electron injection into the conduction band of the TiO_2 nanoparticle in pulse width limited time (< 80 fs). Here, the electron-transfer (< 80 fs) process dominates over the intrinsic exciton-relaxation process (J-aggregates: ca. 200 fs) on account of exciton-coupled CT interaction. The parent hole on J-aggregates is delocalized through J-aggregate excitonic coherence. As a result, holes immobilized on J-aggregates are spatially less accessible to electrons injected into TiO_2, and thus the back electron transfer (BET) process is slower than that of the monomer/TiO_2 system. The J-aggregate/porphyrin system shows exciton spectral and temporal properties for better charge separation in strongly coupled composite systems.

Keywords: aggregation · charge transfer · Frenkel excitons · porphyrins · titania

Introduction

Porphyrin/TiO_2 systems are conjugated π-electron donor–bridge–acceptor materials for dye-sensitized solar cells (DSSC),[1] in which charge separation occurs at the molecular level. In such photovoltaic devices, the multilayer interfacing of molecular species modifies donor levels with exciton coherence.[2] On light absorption, either Frenkel excitons are generated directly at the hetero-interface or diffuse to it, where they dissociate into free charge carriers. In particular, the electron is injected into the conduction band of a semiconductor substrate, while the hole resides on a molecular adsorbate. Hence, interfacial exciton dissociation is of fundamental and practical importance for generation of free charge carriers. Hereby, the function of excitonic solar cells (XSC)[3] is of special interest, due to its close resemblance to the natural chlorophyll 3D light-harvesting antenna[4] system. In such photovoltaic devices, exciton dissociation is conditional to charge-selective contacts in which the thermodynamic requirement is set by the barrier height between exciton levels (donor) and the substrate Fermi level (acceptor). In this regard, TiO_2[5] has proven to be a promising material for solar energy conversion with its high density of states (DOS), low conduction-band (CB) energy, and strong surface linkages, which collectively favor interfacial exciton dissociation. As a counterpart, an ordered porphyrin assembly with its ease of oxidation, high electrochemical activity, and high extinction coefficient is an efficient photosensitizer, particularly for electron injection at the substrate interface.[6] However, the kinetic factors which control interfacial exciton dissociation on a composite material are not very encouraging for the photoconversion process. The problems are exciton motion and its ultrafast decay, which competes with interfacial charge-carrier generation.[7] Furthermore, the weak coupling offered by a nearly perpendicular *meso* phenyl substituent bridge on the porphyrin curbs the coherence of excitons joining the photoconversion process.[8] A substantial criticality arises due to naturally fast decaying excited states (S_2 state ca. 50–300 fs, S_1 state ca. 1–10 ns)[9] of porphyrin monomer, the coherence of which in aggregates further accounts for ultrashort exciton lifetime. The reported exciton lifetimes vary from a few hundred femtoseconds to 100 ps.[10,11b] In addition, the aggregation defect (exciton trap) due to molecular displacement introduces nonradiative loss of photoexcitation energy.[12] These factors collectively restrict porphyrin antenna functionality for interfacial charge-separation phenomenon which also take place in the ultrafast time domain.[13] As a result, porphyrin aggregates are less studied[7,14] due to the complicacy of exciton sensitization. For practical realization, electron transfer from the exciton to the conduction band (CB) of a composite material should take place before the onset of exciton

[a] S. Verma, Dr. H. N. Ghosh
Radiation & Photochemistry Division
Bhabha Atomic Research Centre
Mumbai 400085 (India)
Fax: (+91) 22-25505151
E-mail: hnghosh@barc.gov.in

[b] A. Ghosh, Dr. A. Das
Central Salt & Marine Chemicals Research Institute
Bhavnagar, 364002, Gujarat (India)

Supporting information for this article is available on the WWW under http://dx.doi.org/10.1002/chem.201002537.

decay (intrinsic) or exciton–exciton annihilation,[15] due to the rising exciton concentration in the vicinity. Hence, in the present investigation our major concern is to understand the generation of free charge carriers at a semiconductor (substrate) interface by overruling the ultrafast exciton relaxation processes.

In the present study, we chose porphyrin catechol (TPPcat), which can aggregate and couple with a TiO_2 nanoparticle surface through a *meso*-substituent catechol bridge (Scheme 1). The sensitizer molecule with catecholate moiety

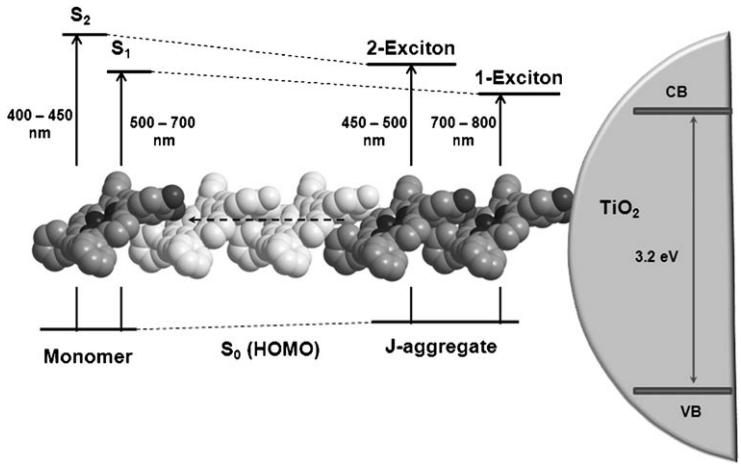

Scheme 1. Schematic diagram of porphyrin J-aggregate/TiO_2 composite. The "head-to-tail" stacking pattern of TPPcat molecules in J-aggregate introduces exciton absorption bands (450–500 and 700–800 nm) into the spectral sensitization of TiO_2 NP.

is known for its strong charge-transfer (CT) complex formation with TiO_2 nanoparticles (NPs).[16,17,18] The cathecol–TiO_2 linkage can favor interfacial dissociation of excitons due to their higher binding energy (ca. 1.15 eV)[19b,c] compared to the exciton binding energy (ca. 0.8–1.0 eV)[19a] of porphyrin aggregates. Thus, catechol-functionalized porphyrin J-aggregates are used to study interfacial exciton dissociation on sensitized TiO_2 NPs. Steady-state absorption, emission, time-correlated single-photon counting (TCSPC), and femtosecond transient absorption spectroscopic studies are employed to understand the exciton spectral and temporal properties in the generation of free charge carriers in porphyrin J-aggregate/TiO_2 systems.

Experimental Section

Materials: Titanium(IV) tetraisopropoxide (Aldrich, 97%), methanol (Aldrich), and isopropyl alcohol (Aldrich) were purified by distillation. Nanopure water (Barnsted System, USA) was used for making aqueous solutions. The synthesis of 5,10,15-trisphenyl-20-(3,4-dihydroxyphenyl) porphyrin (TPPcat) is reported elsewhere.[30] Solvents were degassed thoroughly with IOLAR-grade dinitrogen gas before use in the preparation of all standard solutions.

TiO_2 nanoparticle preparation: Nanometer-sized TiO_2 was prepared by controlled hydrolysis of titanium(IV) tetraisopropoxide.[14] A solution of $Ti[OCH(CH_3)_2]_4$ (5 mL) in isopropyl alcohol (95 mL) was added dropwise (1 mL min^{-1}) to nanopure water (900 mL, 2 °C) at pH 1.5 (adjusted with HNO_3). The solution was continuously stirred for 10–12 h until a transparent colloid was formed. The colloidal solution was concentrated at 35–40 °C with a rotary evaporator and then dried with a nitrogen stream to yield a white powder. In the present work all colloidal samples were prepared after dispersing the dry TiO_2 nanoparticles in water (15 g L^{-1}).

Sample preparation: J-aggregates of TPPcat were prepared at pH 1.8 by following the reported procedure.[31] TPPcat is self-aggregated at pH 1.8 in aqueous HNO_3, whereas TPPcat monomer is stabilized at pH 1.8 in aqueous HCl. J-aggregates of TPPcat were characterized by CD spectra (see the Supporting Information). TiO_2 NPs were sensitized with TPPcat monomers and J-aggregates at pH 1.8, at which J-aggregates are quite stable.

Femtosecond visible spectrometer: The femtosecond tunable visible spectrometer was developed on the basis of a multipass amplified femtosecond Ti:sapphire laser system from Avesta, Russia (1 kHz repetition rate at 800 nm, 50 fs, 800 μJ/pulse) and described earlier.[23] The 800 nm output pulse from the multipass amplifier is split into two parts to generate pump and probe pulses. In the present investigation we used both 800 nm (fundamental) and its frequency double (400 nm) as excitation sources. To generate pump pulses at 400 nm one part of 800 nm with 200 μJ/pulse is frequency-doubled in β-barium borate (BBO) crystals. To generate visible probe pulses, about 3 μJ of the 800 nm beam is focused onto a 1.5 mm-thick sapphire window. The intensity of the 800 nm beam is adjusted by iris size and ND filters to obtain a stable white-light continuum in the 400 to >1000 nm region. The probe pulses are split into signal and reference beams and are detected by two matched photodiodes with variable gain. We kept the spot sizes of the pump beam and probe beam at the crossing point at about 500 and 300 μm, respectively. The excitation energy density (at both 800 and 400 nm) was adjusted to about 2500 μJ cm^{-2}. The noise level of the white light is about 0.5% with occasional spikes due to oscillator fluctuation. We noticed that most laser noise is low-frequency noise and can be eliminated by comparing the adjacent probe laser pulses (pump blocked versus unblocked by using a mechanical chopper). The typical noise in the measured absorbance change is less than about 0.3%. The instrument response function (IRF) for 400 nm excitation was obtained by fitting the rise time for bleaching of the sodium salt of *meso*-tetrakis(4-sulfonatophenyl) porphyrin (TPPS) at 710 nm and found to be about 80 fs.

Results and Discussion

Spectral sensitization: monomer/TiO_2 versus J-aggregate/TiO_2: Figure 1a shows the absorption spectra of the protonated form of TPPcat monomer at pH 1.8 in aqueous HCl solution. It comprises a Soret band ($S_2 \leftarrow S_0$ transition) in the 400–450 nm region and a Q band ($S_1 \leftarrow S_0$ transition) in the 500–700 nm regions. In our earlier work,[31] the unprotonated form of TPPcat monomer was reported to have one strong Soret band at 422 nm and four minor Q-band peaks at 522, 559, 595, and 653 nm. On protonation, the symmetry of the porphyrin molecule changes from D_{2h} to D_{4h}. As a result, the Q band consists only of one strong Q band at 660 nm. At pH 1.8 in HNO_3 aqueous solution, TPPcat forms J-aggregates, which exist in equilibrium with a small amount of the monomeric form. The Soret and Q-exciton bands of J-aggregates are observed in the 460–500 nm (2-exciton) and 700–800 nm (1-exciton) regions (Figure 1c), respectively. On addition of TiO_2 to J-aggregates, the relative increments in Soret and Q-exciton absorption band and remarkably red-shifted absorption in the 800–970 nm region can be attribut-

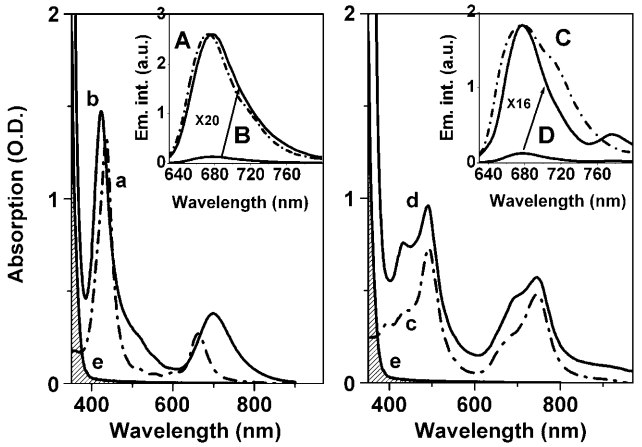

Figure 1. Optical absorption spectra of TPPcat (20 μM) under different conditions: a) monomer , b) monomer/TiO_2, c) J-aggregate, d) J-aggregate/TiO_2, e) bare TiO_2. Inset: Q-band emission spectra of A) monomer, B) monomer/TiO_2, C) J-aggregate, D) J-aggregate/TiO_2.

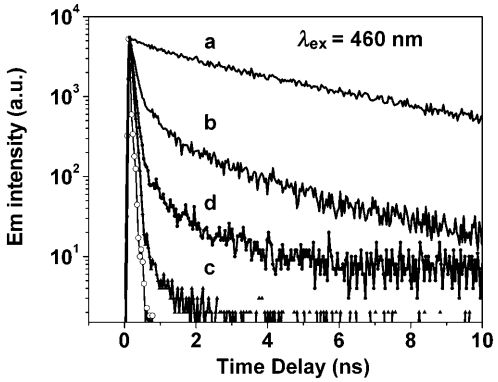

Figure 2. Emission decay traces for the TPPcat (20 μM) with 460 nm (ca. 39 ps full width at half-maximum) excitation wavelength: a) monomer, b) J-aggregate, c) monomer/TiO_2, d) J-aggregate/TiO_2.

ed to exciton-coupled CT complex formation (Figure 1 d). In this integrated J-aggregate/TiO_2 system, preserved exciton spectral properties can be perceived by means of the charge-transfer process at the interface. The presence of an exciton-coupled TiO_2 CT state is reconfirmed by photoluminescence studies (Figure 1 inset and the Supporting Information). Photoexcitation of the above systems facilitates electron transfer from TPPcat (both monomer and J-aggregates) to TiO_2 nanoparticle, whereby we observed a drastic reduction in TPPcat emission. However in the J-aggregate/TiO_2 system, a characteristic redshifted emission is observed at 770 nm and assigned to CT emission[20] (Figure 1 D and the Supporting Information). Here, strong coupling of J-aggregate and TiO_2 NP results in new hybridized states, known as CT states. These CT states are of low energy in comparison to exciton states of the J-aggregate and are confined to the TiO_2 surface.[17] Therefore, the redshifted emission at 770 nm corresponds to direct BET from TiO_2 NPs to J-aggregates of TPPcat. The kinetics of CT recombination are investigated by time-resolved photoluminescence studies (see below).

Time-correlated single-photon counting (TCSPC) measurements: exciton-coupled CT emission: Emission kinetics of TPPcat monomer (Figure 2 a) can be fitted biexponentially with time constants of 2.6 ns (74 %) and 9.2 ns (26 %). However, J-aggregated porphyrin can be fitted biexponentially with much shorter components of 180 ps (85 %) and 2.3 ns (15 %) (Figure 2 b). The major reduced radiative component (180 ps) is assigned to exciton coherence (coherence length $N_c \approx 14$) of S_1 states (Q band).[15] The result has significance as it matches with earlier reported Q-exciton lifetimes (150–300 ps), which rules out the exciton–exciton annihilation process for its short decay profile.[16] Also, it implies that though a small amount of TPPcat monomer exists in equilibrium with J-aggregates, photophysical properties are mainly dominated by temporal exciton properties of J-aggregates. Now, in the TPPcat monomer/TiO_2 system we have observed decay limited by the instrument response (ca. 39 ps, ca. 99.8 %). However, the exciton-coupled CT transition in J-aggregate/TiO_2 NP monitored at 770 nm can be fitted multiexponentially with time constants of 45 ps (98.5 %), 350 ps (1.2 %), and on the order of nanoseconds (0.3 %). Our earlier studies revealed that electron injection in the TPPcat monomer/TiO_2 system (strongly coupled) takes place on a timescale shorter than 50 fs. Hence, the shortest component 45 ps (98.5 %) cannot be attributed to emission quenching. The multicomponent decay profile of the J-aggregate/TiO_2 system can be attributed to the exciton-coupled charge-recombination time between electrons in the conduction band of TiO_2 and excitonic holes in J-aggregates. The observance of CT emission confirms direct involvement of exciton coherence in interfacial charge separation phenomena, which otherwise sees a diffusion-limited loss of exciton states.[27] It implies significant mixing of exciton states of J-aggregates and charge-transfer states of terminal TPPcat/TiO_2 coupling in the J-aggregate/TiO_2 system. Therefore, photoinduced charge separation can follow a dynamic delocalization while relaxing along exciton and CT potential surfaces.[29] Thus, charge-carrier hopping is expected to be redefined in the system and further investigated by transient absorption (TA) pump–probe spectroscopy.

Transient absorption (TA) measurements: monomer/TiO_2 versus J-aggregate/TiO_2: The transient absorption spectra and related kinetics of TPPcat monomer, TPPcat monomer/TiO_2, and J-aggregate of TPPcat are explained in Figures S3–S8 of the Supporting Information. Here the TA spectra and kinetics are presented for direct comparison of interfacial electron-transfer (IET) dynamics in monomer/TiO_2 versus J-aggregate/TiO_2 system.

The TA studies are carried out at 400 nm excitation wavelength, which is the only available excitation wavelength in the current pump–probe absorption spectrometer. Figure 3 shows the TA spectra of monomer/TiO_2 and J-aggregate/TiO_2 at pH 1.8. Comparison of Figure 3 A and 3 B reveals a new bleach band in the 470–520 nm region and an increased

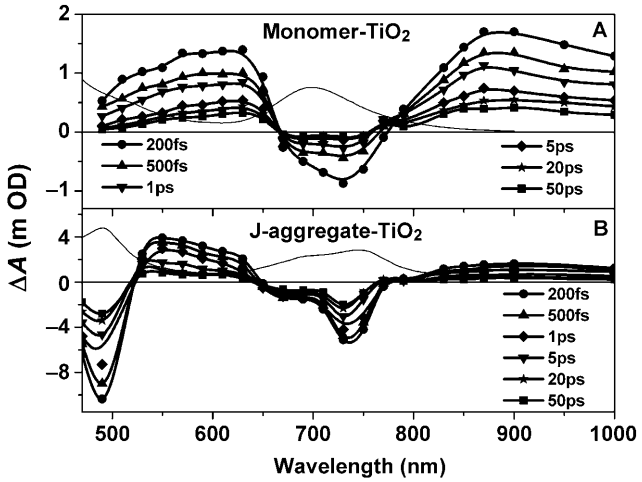

Figure 3. Transient absorption spectra of monomer/TiO_2 NP (A) and J-aggregate/TiO_2 NP (B) at different time delays after excitation with 400 nm laser light. Steady-state absorption is shown for comparison (thin line).

bleach band in the 710–770 nm region representing the Soret- and Q-exciton-coupled CT absorption band of the J-aggregate/TiO_2 system (Figure 1d). The positive absorption band in the 800–1000 nm region can be assigned to electrons in the conduction band of TiO_2 NPs. The broad TA band in the 520–630 nm region can be attributed to oxidized J-aggregate/TPPcat species formed immediately after electron injection from photoexcited J-aggregate/TPPcat into the TiO_2 CB. Thus, the exciton-coupled CT dynamics (J-aggregate/TiO_2) are studied by bleach recovery dynamics at the corresponding exciton bleach bands (490 and 750 nm), whereas the electron transfer dynamics are studied at 1000 nm probe wavelength.

Figure 4 shows the normalized kinetics at 1000 nm for injected electrons (e^- CB) and at 670 nm (bleach kinetics resembling the BET process) for both monomer- and J-aggregate-sensitized TiO_2 nanoparticles. The appearance signal at 1000 nm for e^- CB in both TPPcat monomer/TiO_2 and J-aggregate/TiO_2 systems were found to be pulse width limited (<80 fs) and confirms strong coupling between porphyrin and TiO_2. Earlier we demonstrated that sensitizer molecules (ruthenium and osmium polypyridyl complexes) with catecholate binding to the TiO_2 nanoparticle surface exhibit ultrafast electron injection from unthermalized states.[23] We have also reported that strong coupling of the TPPcat-monomer-sensitized TiO_2 system facilitates electron injection from vibrationally hot S_2 or S_1 states simultaneously.[24] In TPPcat monomer (in the absence of TiO_2), an instantaneous (pulse-width-limited) $S_2 \rightarrow S_1$ internal conversion (IC) results in the unthermalized Q-excited (S_1) state which subsequently thermalized in a biphasic[25,26b] vibrational relaxation process (ca. 4 ps and ca. 20 ps; Supporting Information). However, in presence of TiO_2 NP, the ultrafast electron injection from unthermalized S_2 or S_1 state cease this biphasic vibrational relaxation and an instantaneous bleach signal is observed at 670 nm (Figure 4c). In the case of J-aggregates (in absence of TiO_2), the excitonic coupling between Soret- and Q-excitonic bands is expected to further influence the IC process more rapidly and efficiently.[11] Furthermore, on J-aggregation, the coherence of the S_2 and S_1 states drastically reduces their lifetimes to 200 fs and 180 ps, respectively (see the Supporting Information). Interestingly, in the J-aggregate/TiO_2 system, the strong coupling between terminal TPPcat and TiO_2 facilitates ultrafast electron injection (<80 fs) from respective exciton states before onset of their own (intrinsic) exciton relaxation process (see the Supporting Information). As a result, the Soret- and Q-exciton relaxation (200 fs and 180 ps) components are absent in Soret- and Q-exciton bleach recovery (490, 670, 730 nm) in the J-aggregate/TiO_2 system (Figure 4; see also the Supporting Information). This observation clearly indicates that both excitonic states are able to inject electron in TiO_2 CB while leaving behind a hole on J-aggregate of TPPcat.

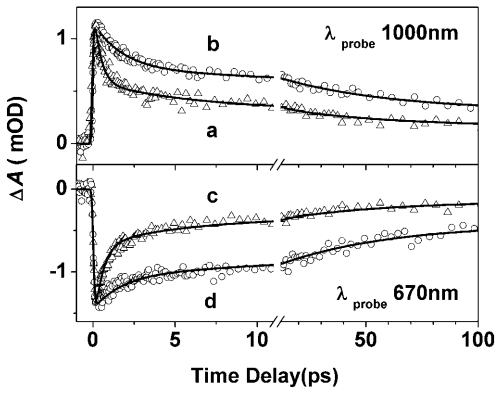

Figure 4. Normalized kinetic traces of electrons injected into the CB of TiO_2 at 1000 nm in a) monomer/TiO_2 system, b) J-aggregate/TiO_2 system and normalized bleach recovery kinetics in c) monomer/TiO_2, d) J-aggregate/TiO_2 at 670 nm.

The charge separation which took place after pulse width limited electron injection at the dye (or J-aggregate)/TiO_2 interface is subject to recombination in due course and finally regenerates the ground state of the dye (or J-aggregate)-TiO_2 system. In a strongly coupled CT system the injected electron can be localized at the TiO_2 surface due to strong CT interaction or delocalized in the conduction band (high density of states) of TiO_2. Therefore, the recombination dynamics is accordingly contributed by localized and delocalized electron very distinctly. We determined BET dynamics by monitoring the transient signal at 1000 nm or bleach recovery kinetics at 670 nm. In the present studies we observed a slower BET dynamics (670 nm) in J-aggregate/TiO_2 system [1.8 ps (27.8%), 50 ps (41.1%), >ns (31.1%)] with respect to the monomer TPPcat/TiO_2 system [400 fs (63.6%), 5 ps (13.3%), 50 ps (13.3%), >ns (10.8%)]. This might be due to location of the hole (oxidized TPPcat) on the sole TPPcat molecule, which couples strongly with the TiO_2 nanoparticle in case of the monomer TPPcat/TiO_2 system. As a result, the injected electron in the TiO_2 NP has significant chance for recombination. On the contrary, in the case of J-aggregate/TiO_2, due to local field modification in

the TPPcat building units within the J-aggregate, highly delocalized Soret and Q-exciton states are generated whereby the HOMO (exciton) level of the J-aggregate is energetically higher than the HOMO level of TPPcat monomer.[5b] Now on photoexcitation of excitonic states, the exciton motion, which is coherent within coherence length on approaching the TiO_2 NP, reaches to terminal TPPcat (bound to TiO_2 surface) where strong coupling results in an efficient and ultrafast charge separation at the interface. The hole produced after electron injection is no longer bound to terminal TPPcat (closest to TiO_2 NP surface) and migrates away from the J-aggregate/TiO_2 interface via the high-lying exciton HOMO of the J-aggregate. Incoherent hole hopping[26] between adjacent porphyrin units is reported to take place on the subnanosecond time domain. However in the present investigation, the J-aggregate comprises coherent HOMO levels of many TPPcat units, and hence the hole-hopping rate can be on the order of the subpicosecond timescale.[27] Therefore, due to fast hole hopping following pulse width limited (<50 fs) electron injection, better spatial charge separation takes place at the interface. As a result, the BET process is slowed down in the J-aggregate/TiO_2 system compared to the TPPcat monomer/TiO_2 system (Scheme 2). This is one way in which exciton coherence leads to better charge separation at the J-aggregate/TiO_2 interface.

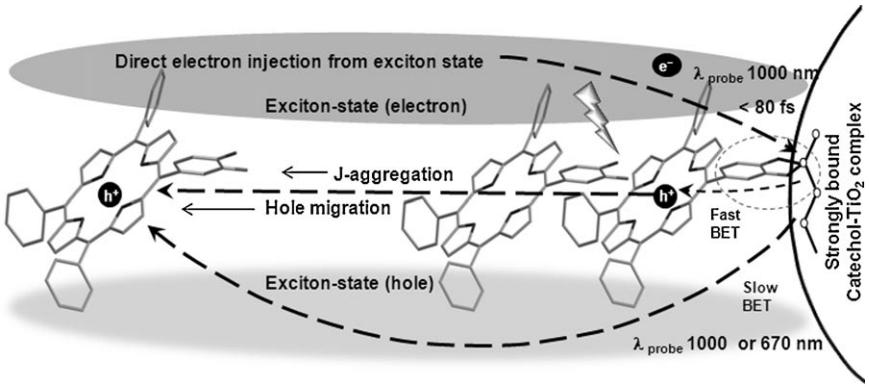

Scheme 2. Free charge-carrier generation in Frenkel exciton-coupled porphyrin J-aggregate/semiconductor (TiO_2) composite system, accomplished through an interfacial exciton-dissociation process. The separated hole is delocalized through excitonic coherence of the J-aggregate. The immobilized hole is spatially less accessible to electrons injected into TiO_2 and hence leads to slower BET.

In our earlier studies,[24] we observed that in the blue region (400–600 nm) of the TA spectra of the TPPcat monomer/TiO_2 system, the dynamics are dominated by the characteristics of the pure catechol/TiO_2 CT complex. The TA kinetics monitored at these wavelengths (e.g., 570 nm, see the Supporting Information) gives an additional fast component of 130 fs (major, 67%) in addition to the other components (400 fs, 5 ps, 50 ps, longer than nanoseconds) observed at 1000 nm decay kinetics. Recent hybrid B3LYP DFT calculations on the TPPcat system[28] showed that catechol moiety is appended nearly perpendicularly (dihedral angle 112.8°) to the porphyrin ring. In such a geometrical configuration, the catechol moiety no longer remains in full conjugation with the porphyrin π-electron system, and has its own HOMO, which in fact constitutes the initial state of the excited state that later turns into the LUMO, primarily contributed by the porphyrin ring. Therefore, in the presence of unfulfilled valence surface states of TiO_2 NP, significant hybridization occurs with molecular orbitals of only the catechol moiety, which form the basis of an additional catechol/TiO_2 CT absorption band (Figure 1b) in the 400–600 nm region. Furthermore, a nearly perpendicular orientation of *meso*-substituent anchor rings, be they carboxylate, sulfate, phosphate, or catechol binding groups, imposes a lower electronic coupling between porphyrin ring and TiO_2 NP, as was pointed out earlier by Bignozzi et al.[8] Therefore, in this situation a significant catechol–TiO_2 CT band will interfere with porphyrin–TiO_2 electronic coupling. Earlier Lian and co-workers carried out TA studies on the pure catechol/TiO_2 system,[29] where they reported an ultrafast component (ca. 400 fs, ca. 60%) in the TA decay kinetics. The ultrafast component was attributed to charge-recombination dynamics of localized electrons (TiO_2) and catechol cations. Similarly, in the present investigation, the additional ultrafast decay component (130 fs) observed in the blue region of TA spectra of the TPPcat monomer/TiO_2 system can be attributed to direct charge recombination of localized electrons which has catechol/TiO_2 CT character.[29,18] However, TA kinetics monitored at 1000 nm does not show this ultrafast component and can be attributed to the recombination kinetics of delocalized electron (TiO_2 CB) and TPPcat cation.[24,14] In the case of the J-aggregate/TiO_2 system, only terminal TPPcat could inherit this extra CT complex (pure catechol/TiO_2), while most of TPPcat molecules are stacked in the head-to-tail configuration of J-aggregates and hence devoid of direct catechol-assisted CT complex formation. At the same time, the exciton coherence of J-aggregates involves many TPPcat (coherence length $N_c \approx 14$ units), which facilitates electron injection into TiO_2 CB after photoexcitation of any constituent porphyrin unit. Thus, on J aggregation, the optically allowed exciton states, with their large oscillator strength in the 400–800 nm region, suppress the absorption of the pure catechol/TiO_2 CT complex (400–600 nm).

We compared the bleach recovery kinetics at 730 nm for both monomer/TiO_2 and J-aggregate/TiO_2 systems (Figure 5). The kinetics data can be fitted multiexponentially with time constants of 500 fs (40%), 2.4 ps (16%), 40 ps (16%), and longer than nanoseconds (22%) for J-aggregate/

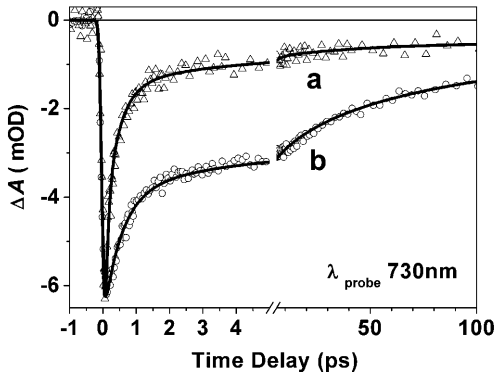

Figure 5. CT kinetics of a) TPPcat monomer/TiO_2, b) TPPcat J-aggregate/TiO_2 at 730 nm.

TiO_2 and 100 fs (54%), 400 fs (29.1%), 3 ps (5.8%), 50 ps (3%), and longer than nanoseconds (8.1%) for TPPcat monomer/TiO_2. Interestingly, the 100 fs component is missing in the J-aggregate/TiO_2 system. Considering the strong coupling offered by the catecholate moiety, this is a remarkable observation in the ET dynamics of the J-aggregate/TiO_2 system. In J-aggregates, the Q_x (or B_x) transition moments of many TPPcat units (constituting the "head-to-tail" pattern along the J-aggregation axis) interact strongly to produce exciton states with their **k** (exciton) vector oriented in the direction of the TiO_2 CB acceptor states. On TiO_2 NP surface, the J-aggregates retain these coherent excited states (excitons) and sensitize them as a single entity via their terminal TPPcat groups, and this results in a J-aggregate/TiO_2 CT complex. The J-aggregate/TiO_2 CT complex was pointed out in the above steady-state absorption and emission studies. Hence, the shortest component of 500 fs in the bleach recovery dynamics at 730 nm is assigned to the exciton-coupled CT transition of the J-aggregate TPPcat/TiO_2 system. In this case, the bleach recovery kinetics at 730 nm represents recombination dynamics of localized electron and cation of the J-aggregate. This phenomenon is further reconfirmed by the 570 nm TA decay profile of monomer/TiO_2 versus J-aggregate/TiO_2 system (Figure S8, Supporting Information).

Conclusion

We have demonstrated charge-carrier generation in the exciton-coupled charge-transfer complex between J-aggregates of TPPcat and TiO_2 NPs. In the J-aggregate/TiO_2 system, ultrafast ET dominates over fast exciton relaxation of J-aggregates. Also, the exciton transitions with very large oscillator strength owing to many optically allowed coherent excited states (exciton) in J-aggregates/TiO_2 increase the delocalized electron injection yield (ca. 15%) in the CB of TiO_2 compared to the monomer/TiO_2 system. The hole generated after interfacial exciton dissociation is delocalized through exciton coherence, which increases the spatial charge separation. For that reason, the charge-recombination dynamics is found to be drastically slowed down in the J-aggregate/TiO_2 system compared to the TPPcat monomer/TiO_2 system. Our results clearly demonstrate that the location of positive charges (holes) in sensitizer/nanoparticle systems influences the charge-recombination dynamics significantly even in a strongly coupling system. The study shows that the antenna functionality of circular aggregates and primary charge separation at the interface (reaction center) can be coupled in favor of efficient charge-carrier generation (electron/hole) in photon-processing units. The large exciton binding energy and ultrafast exciton decay processes (ca. 200 fs) are the limiting factor for the exciton-harvesting route. In such systems, the coupling strength dictates the conversion efficiency of charge-neutral exciton states to charge-separated states. The exciton dissociation at the interface is gained from strong binding energy (catechol–TiO_2), and thus strong coupling reinstates the electron-transfer (<80 fs) process at the interface.

Acknowledgements

We thank Dr. T. Mukherjee, and Dr. S. K. Sarkar of BARC, and Dr. P. K. Ghosh of CSMCRI for their constant encouragement. H.N.G. thanks BRNS, while A.D. thanks DST and BRNS for financial assistance.

[1] a) C.-W. Lee, H.-P. Lu, C.-M. Lan, Y.-L. Huang, Y.-R. Liang, W.-N. Yen, Y.-C. Liu, Y.-S. Lin, E. W.-G. Diau, C.-Y. Yeh, *Chem. Eur. J.* **2009**, *15*, 1403; b) R. Ma, P. Guo, H. Cui, X. Zhang, M. K. Nazeeruddin, M. Grätzel, *J. Phys. Chem. A* **2009**, *113*, 10119; c) H. Imahori, T. Umeyama, S. Ito, *Acc. Chem. Res.* **2009**, *42*, 1809; d) A. Mishra, M. K. R. Fischer, P. Bäuerle, *Angew. Chem.* **2009**, *121*, 2510; *Angew. Chem. Int. Ed.* **2009**, *48*, 2474.

[2] a) J. M. Ribó, J. M. Bofill, J. Crusats, R. Rubires, *Chem. Eur. J.* **2001**, *7*, 2733; b) H. Fidder, J. Knoester, D. A. Wiersma, *J. Chem. Phys.* **1991**, *95*, 7880.

[3] B. A. Gregg, *J. Phys. Chem. B* **2003**, *107*, 4688.

[4] R. M. Pearlstein, *Photosynth. Res.* **1996**, *48*, 75.

[5] D. F. Watson, G. J. Meyer, *Annu. Rev. Phys. Chem.* **2005**, *56*, 119.

[6] a) Y. He, E. Borguet, *Angew. Chem. Int. Ed.* **2007**, *46*, 6098; b) A. Takai, C. P. Gros, J.-M. Barbe, R. Guilard, S. Fukuzumi, *Chem. Eur. J.* **2009**, *15*, 3110.

[7] a) A. Huijser, B. M. J. M. Suijkerbuijk, R. J. M. K. Gebbink, T. J. Savenije, L. D. A. Siebbeles, *J. Am. Chem. Soc.* **2008**, *130*, 2485; b) L. Luo, C. F. Lo, C. Lin, I. Chang, E. W. Diau, *J. Phys. Chem. B* **2006**, *110*, 410; c) A. Huijser, T. J. Savenije, J. E. Kroeze, L. D. A. Siebbeles, *J. Phys. Chem. B* **2005**, *109*, 20166.

[8] F. Odobel, E. Blart, M. Lagre'e, M. Villieras, H. Boujtita, N. E. Murr, S. Caramoric, C. A. Bignozzi, *J. Mater. Chem.* **2003**, *13*, 502.

[9] a) M. Enescu, K. Steenkeste, F. Tfibel, M.-P. Fontaine-Aupart, *Phys. Chem. Chem. Phys.* **2002**, *4*, 6092; b) A. Marcelli, P. Foggi, L. Moroni, C. Gellini, P. R. Salvi, I. J. Badovinac, *J. Phys. Chem. A* **2007**, *111*, 2276.

[10] a) H. Kano, T. Kobayashi, *J. Chem. Phys.* **2002**, *116*, 184; b) E. Collini, C. Ferrante, R. Bozio, *J. Phys. Chem. C* **2007**, *111*, 18636.

[11] a) J. Zimmermann, U. Siggel, J. H. Fuhrhop, B. Röder, *J. Phys. Chem. B* **2003**, *107*, 6019; b) H. Kano, T. Saito, T. Kobayashi, *J. Phys. Chem. A* **2002**, *106*, 3445.

[12] a) S. M. Vlaming, R. Augulis, M. C. A. Stuart, J. Knoester, P. H. M. van Loosdrecht, *J. Phys. Chem. B* **2009**, *113*, 2273; b) A. V. Sorokin, I. I. Filimonova, R. S. Grynyov, G. Y. Guralchuk, S. L. Yefimova, Y. V. Malyukin, *J. Phys. Chem. C* **2010**, *114*, 1299; c) V. Gulbinasa,

R. Karpicza, R. Augulisc, R. Rotomskisc, *Chem. Phys.* **2007**, *332*, 255.
[13] Y. Tachibana, J. E. Moser, M. Grätzel, D. R. Klug, J. R. Durrant, *J. Phys. Chem.* **1996**, *100*, 20056.
[14] a) C.-W. Chang, L. Luo, C.-K. Chou, C.-F. Lo, C.-Y. Lin, C.-S. Hung, Y.-P. Lee, E. W.-G. Diau, *J. Phys. Chem. C* **2009**, *113*, 11524.
[15] a) M. R. Wasielewski, *Chem. Rev.* **1992**, *92*, 435; b) V. Sundström, T. Gillbro, R. A. Gadonas, A. Piskarskas, *J. Chem. Phys.* **1988**, *89*, 2754.
[16] a) P. Persson, R. Bergström, S. Lune, *J. Phys. Chem. B* **2000**, *104*, 10348; b) T. Lana-Villarreal, A. Rodes, J. M. Pérez, R. Gómez, *J. Am. Chem. Soc.* **2005**, *127*, 12601; c) G. Ramakrishna, A. K. Singh, D. K. Palit, H. N. Ghosh, *J. Phys. Chem. B* **2004**, *108*, 1701.
[17] O. V. Prezhdo, W. R. Duncan, V. V. Prezhdo, *Prog. Surf. Sci.* **2009**, *84*, 30.
[18] L. Gundlach, R. Ernstorfer, F. Willig, *Phys. Rev. B* **2006**, *74*, 035324.
[19] a) X.-F. Ren, A.-M. Ren, J.-K. Feng, X. Zhou, *Org. Electron.* **2010**, *11*, 979; b) S.-C. Li, L.-N. Chu, X.-Q. Gong, U. Diebold, *Science* **2010**, *328*, 882; c) P. C. Redfern, P. Zapol, L. A. Curtiss, T. Rajh, M. C. Thurnauer, *J. Phys. Chem. B* **2003**, *107*, 11419.
[20] a) H. N. Ghosh, *J. Phys. Chem. B* **1999**, *103*, 10382; b) S. Verma, P. Kar, A. Das, D. K. Palit, H. N. Ghosh, *J. Phys. Chem. C* **2008**, *112*, 2918.
[21] a) J. E. Kroeze, R. B. M. Koehorst, T. J. Savenije, *Adv. Funct. Mater.* **2004**, *14*, 992; b) J. E. Kroeze, T. J. Savenije, J. M. Warman, *Adv. Mater.* **2002**, *14*, 1760.
[22] a) R. J. Cave, P. Siders, R. A. Marcus, *J. Phys. Chem.* **1986**, *90*, 1436; b) T. H. Tran-Thi, J. F. Lipskier, P. Mailard, M. Momenteau, J. M. Lopez-Castillo, J. P. Jay-Gerin, *J. Phys. Chem.* **1992**, *96*, 1073.
[23] a) G. Ramakrishna, D. A. Jose, D. K. Kumar, A. Das, D. K. Palit, H. N. Ghosh, *J. Phys. Chem. B* **2005**, *109*, 15445; b) S. Verma, P. Kar, A. Das, D. K. Palit, H. N. Ghosh, *Chem. Eur. J.* **2010**, *16*, 611.
[24] G. Ramakrishna, S. Verma, D. A. Jose, D. K. Kumar, A. Das, D. K. Palit, H. N. Ghosh, *J. Phys. Chem. B* **2006**, *110*, 9012.
[25] J. S. Baskin, H. Z. Yu, A. H. Zewail, *J. Phys. Chem. A* **2002**, *106*, 9837.
[26] a) I.-W. Hwang, M. Park, T. K. Ahn, Z. S. Yoon, D. M. Ko, D. Kim, F. Ito, Y. Ishibashi, S. R. Khan, Y. Nagasawa, H. Miyasaka, C. Ikeda, R. Takahashi, K. Ogawa, A. Satake, Y. Kobuke, *Chem. Eur. J.* **2005**, *11*, 3753; b) Y. H. Kim, D. H. Jeong, D. Kim, S. C. Jeoung, H. S. Cho, S. K. Kim, N. Aratani, A. Osuka, *J. Am. Chem. Soc.* **2001**, *123*, 76.
[27] D. Holten, D. F. Bocian, J. S. Lindsey, *Acc. Chem. Res.* **2002**, *35*, 57.
[28] C.-R. Zhang, Y.-H. Chen, Z.-S. Pu, Z.-Q. Wei, D.-B. Wang, Y.-Z. Wu, H.-S. Chen, *J. Atom. Mol. Phys.* **2008**, issue *5*, 1241.
[29] Y. Wang, K. Hang, N. A. Anderson, T. Lian, *J. Phys. Chem. B* **2003**, *107*, 9434.
[30] A. D. Jose, A. D. Shukla, . D. Krishnakumar, B. Ganguly, A. Das, G. Ramakrishna, D. K. Palit, H. N. Ghosh, *Inorg. Chem.* **2005**, *44*, 2414.
[31] S. Verma, A. Ghosh, A. Das, H. N. Ghosh, *J. Phys. Chem. B* **2010**, *114*, 8327.

Received: September 2, 2010
Published online: February 15, 2011

